Influence of Fabric Structural Attributes on Their Aerodynamic Behavior

Lars Morten Bardal, Luca Oggiano, Olga Troynikov, Inna Konopov

Norwegian University of Science and Technology (NTNU), Trondheim NORWAY

Correspondence to:
Lars Morten Bardal email: lars.m.bardal@ntnu.no

ABSTRACT

The aerodynamic properties of 15 knitted fabrics of varying cover factor, yarn, and fiber compositions were investigated for their aerodynamic properties on circular cylinders in a wind tunnel. Measurements of the drag force, pressure distribution, and the Particle Image Velocimetry (PIV) technique were used in order to obtain a better understanding of the effects of yarn, fiber composition, cover factor, and elastic deformation on the flow field and drag coefficient. It was clearly demonstrated from the drag force measurements that the yarn construction and fiber composition have a substantial effect on the drag coefficient (C_D), with fabrics composed of spun yarn experiencing no C_D-drop as opposed to those composed of filament yarn, and being almost unaffected by the cover factor in the range of Reynolds numbers investigated. Hairiness of the spun yarn was found to minimise the drag-reducing effect of the boundary layer transition and increase the trans-critical drag. The hairy surface layer also appeared to retard the turbulent boundary layer as almost no pressure recovery was observed prior to separation on the cylinder model.

The effect of elastic deformation was investigated by image analysis of scanned textile samples, and demonstrated that surface roughness might not be directly correlated to cover factor when the fabrics are stretched. Different elastic behavior of fabrics with different cover factors was also found to affect the structure of the knit surface and thus their aerodynamic behavior. The onset of drag crisis found in drag measurements confirmed the deviation from a sequence determined solely by cover factor.

INTRODUCTION

As the speed margins in top-level competitive athletics become smaller with every event, the influence of factors outside the athletes themselves become more important. Through the last two decades research in sports technology has become increasingly critical for the improvement of sports performance, and is now a key factor in the pursuit of new records. In many typical high speed sports such as speed skating, alpine skiing, road cycling, and sprint running, the time margins between victory and a mediocre performance is often just a few thousandths of the total competition time. In such sports a major part of the athlete's force is used to overcome wind resistance, for example in field cycling it is typically 90% [1], and in speed skating is more than 75%[2]. This percentage will also increase further as the speed increases, since wind resistance is dependent on the speed squared. Therefore it is fair to assume that even a small improvement in the aerodynamic properties of the athlete can cause a considerable enhancement of performance, and perhaps the largest potential of improvement lies in the sports apparel.

The favourable effects of surface roughness and air permeability of fabrics on air flow have already been utilised in sports apparel for a number of sports in order to lower the aerodynamic drag [3, 4]. A common approach is to design zoned skin suits where different textile materials are integrated into the suits according to their position on the relevant body parts. Brownlie et al. developed a time trial cycling suit with this approach using a variety of different fabrics and also streamlining and reducing the number of seams [5]. They claimed to achieve a drag reduction of 3.9 per cent compared to a standard cycling suit. This approach has also been successfully used on loose fitting apparel [6] as well for speed skating and running suits.

The drag force acting on any body moving through a fluid can be written as

$$D = C_D A \frac{1}{2} \rho U^2 \quad (1)$$

where C_D is a dimensionless drag coefficient, A is the reference area, ρ is the density of the fluid and U is the free stream velocity. For incompressible flows C_D

depends on the Reynolds number Re ($\frac{UD}{\nu}$), the shape of the body, and the surface texture of the body. In order to reduce drag force on an object with a given size and shape in a given environment, such as an athlete moving through air, one consequently needs to manipulate the surface itself. The drag force acting on a body is generally divided into two components: friction drag and pressure drag. Friction drag is the drag component caused by viscous stresses acting on the surface in the boundary layer. For bluff bodies this only accounts for a small fraction (0.75-1.5%) of the total drag for a smooth cylinder in the Reynolds range considered [7]. When the boundary layer separates from the surface of the body far upstream of the trailing edge, it causes a low pressure wake behind the body, and thus the pressure drag becomes the dominant component out of the two. This is the general case of airflow around a human body. Pressure drag is caused by the pressure difference between the windward and leeward side of the body, and thus a reduction in the size of the low pressure wake behind the body would contribute to a reduction in drag. A way to achieve this without tempering with the geometry of the body itself is to manipulate the state of the viscous boundary layer.

A simplified model of the human limbs is a cylinder of circular cross-section [8]. The flow around a cylinder is highly complex and has been widely investigated in the field of fluid dynamics [7, 9-13]. Wieselsberger demonstrated the influence of Reynolds number (Re) on C_D of a circular cylinder, finding a distinct drop in C_D at Re around 2×10^5 [9]. This is now referred to in literature as the "drag crisis". The study also linked this phenomena to the presence of turbulent eddies in the boundary layer which increases boundary layer momentum and consequently the ability of the boundary layer to overcome the adverse pressure gradient of the flow. The effect of artificially created turbulence, both in the free stream and in the boundary layer itself, on the drag coefficient was studied by Fage and Warsap. Their results showed that both surface roughness and free stream turbulence would shift the drag crisis to a lower Reynolds number [10]. The drop in C_D would however seem to be reduced when increasing surface roughness while opposing behavior can be found for artificially created free stream turbulence. This is explained by the fact that increased roughness causes earlier flow separation [11]. Achenbach measured the position of the separation point as a function of the Reynolds number using a skin friction probe and confirmed the assumption that the drag crisis was related to the downstream shift of the separation point and hence the size of the wake [7]. With further increasing Reynolds numbers the separation point will move upstream towards the stagnation point and the final transcritical C_D value will also depend on the roughness [11]. The classification of the basic high level flow regimes in a typical C_D-Re curve is marked in *Figure 1*.

Even though the idealized flow around smooth circular cylinders is found to be dependent on the Reynolds number as a single governing parameter, the different transition states are very sensitive to flow disturbances. In addition possible influencing parameters are free stream turbulence, surface roughness, aspect ratio of the model (diameter vs. length), flow restrictions, oscillations and more. Dependent on their magnitude these parameters can become governing for the flow in some regions [14]. It must therefore be considered that the aerodynamics of sports apparel in practical use will be significantly influenced by these parameters, and should also be tested in a realistic environment.

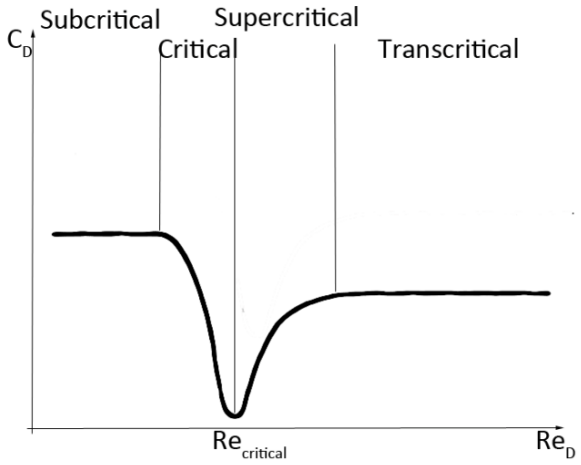

FIGURE 1. Flow regimes of a typical C_D-Re curve.

The present study focuses on the effects of knitted textile fabrics applied as surface roughness, on air flow around circular cylinder models. The effective engineering of new custom fitted aerodynamic sports apparel depends on thorough investigation of new textile materials, and more importantly, on more detailed knowledge of their ability to manipulate the flow field around a bluff body, where bluff bodies are non-streamlined bodies whose drag is mostly caused by flow separation. The influence of other parameters such as 3D effects, caused by posture of an athlete and limb interaction, and free stream turbulence in the real environment must however be taken into account [15]. Fabrics used for clothing can generally be divided into woven and knitted fabrics. Both are made from yarn, but their manufacturing methods are

fundamentally different. In knitted fabrics the yarn is knitted into loops (stitches) which are generally easily deformable regardless of yarn structure and composition. Woven fabrics, on the other hand, are made from orthogonally oriented warp and weft yarns which are interlaced together. This makes the fabric generally non-stretchable unless elastic yarn/fiber is used. This fundamental difference makes knitted fabrics favorable in form fitting apparel such as aerodynamic sports apparel. The aerodynamic properties of the fabrics depend on the air permeability and on the roughness of its resultant surface and are set by the following factors:

- Manufacturing method (structure)
- Yarn count (thickness), Tex
- Yarn/fiber composition
- Yarn construction
- Fabric density
- Cover factor (CF)
- Elastic properties and practical elastic deformation

where the yarn count is a measure for mass per unit length of yarn and the cover factor (CF) is the ratio between the area covered by yarn and the total area of the fabric, defined as

$$CF^2 = \frac{Tex}{L^2} \tag{2}$$

for knitted fabrics of similar structure [16], where Tex is the yarn count and L is the loop length. Cover factor (CF) is also called tightness factor and is a measure for the tightness of the fabric. It is a useful parameter for describing the physical appearance of the knitted fabric, and since it links yarn and fabric parameters into a single parameter it will be used as the fabric variable characteristic in this study.

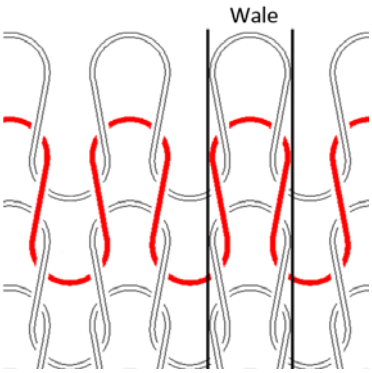

FIGURE 2. Single jersey knit pattern schematic.

Figure 2 shows the structure of the single jersey fabric used in this study. As a consequence of the three dimensionality of the knitted structure, its surface will be elevated at the points of loop intersections and produce a somewhat directional ribbed surface with "ridges" oriented in the wale direction. This will make the surface appear rougher than a similarly homogenous woven fabric. The nature of the yarn is also an influencing parameter on the surface and thus on the aerodynamic characteristics of the fabric. We can distinguish between spun yarn and continuous filament yarn. Spun yarn is made by spinning relatively short staple fiber ends together to form a continuous tread while filament yarn is made from one (mono-filament) or several (multi-filament) continuous filaments twisted together. Filament yarn will have a more or less smooth surface, while spun yarn will have protruding fiber ends making the surface rougher. The effects of such protruding fibers covering the surface was examined by Metha and Pallis on the flow around tennis balls[17]. They found the influence of the "fuzz " on the surface of tennis balls to be more effective not only in triggering transition in the boundary layer at lower than expected Reynolds numbers, but also increasing the total drag with an additional drag component being denoted "fuzz drag". This effect was found to be more pronounced at lower velocities because of increased streamlining of the fiber ends along the flow with increasing speed.

Unlike the surface roughness described by the height of the protruding roughness elements, such as for example in emery paper, there is no obvious parameter to describe the roughness of a textile material. An attempt was made by Oggiano et al. to define the roughness using a two-dimensional simplification of the fabric surface [18]. A general and reliable parameter is however difficult to define because of the variations in loop shape with cover factor and stretch, and also because of the effects of yarn "fuzziness". Another approach is to characterise an equivalent roughness value for roughness of different nature using an empirical formula based on the value of $Re_{critical}$ [19]. In this study no attempt is made to define a roughness parameter, and the samples will be categorized by their yarn material and cover factor.

The pressure drag on a cylinder is only dependent on the pressure distribution around the cylinder surface and can be found by surface integration of the pressure in the direction of the flow. Use of discrete pressure taps located around the cylinder circumference at half-length is a common method for

determination of the pressure distribution, assuming 2D flow conditions. However, in the case of textile clad cylinders, the influence of the textile on the pressure readings is a source of uncertainty. The only relevant reference found was still able to get consistent readings using skin suits on a mannequin doll [15]. Force balance and pressure data as well as particle image velocimetry (PIV) flow field images are acquired in this study to ensure a good basis of comparison.

EXPERIMENTAL

Materials

Single Jersey knitted fabrics constructed of four different yarns and fiber compositions were produced and tested on cylinder shapes in wind tunnel experiments. Wool, cotton, and spun polyester fabrics were made from spun yarn while the other lot of polyester fabrics was made from filament yarn. Fabrics produced with spun yarn will have a number of loose fiber ends protruding from the surface due to the discontinuity of the fibers from which the yarn is built. These loose ends are protruding up to approximately 1mm from the surface giving it a softer feel, and will be denoted as "fuzz" later in the article. All fabric samples were produced on a Lawson Hemphill FAK-S knitting machine at the RMIT University, Melbourne, Australia. The use of this machine allowed for the precise incremental variation of fabric's stitch length and CF as per experimental design. This would be harder to achieve on a commercial multi-feed knitting machine of a large diameter. Fabric samples were knitted in a plain single jersey structure, and the technical front was facing the wind during the experiments.

TABLE I. Fabric sample physical properties.

Fabric sample	Cover factor	Fiber composition	Yarn construction	Yarn count (Tex)	Thickness (mm)	Mass per unit area (g/m^2)
					AS 2001.2.12-1989	AS 2001.2.6-2001
PM1.0	1.0	Polyester	Multifilament	17	0.49	107.5
PM1.2	1.2				0.50	128.3
PM1.3	1.3				0.52	135.8
PM1.4	1.4				0.54	145.0
PS1.0	1.0		Spun	17	0.45	91.7
PS1.2	1.2				0.47	117.6
PS1.3	1.3				0.47	122.0
PS1.4	1.4				0.52	131.7
WS1.0	1.0	Wool		18	0.43	97.3
WS1.2	1.2				0.45	123.7
WS1.3	1.3				0.46	134.3
WS1.4	1.4				0.47	146.0
CS1.0	1.0	Cotton		15	0.46	101.3
CS1.2	1.2				0.52	117.0
CS1.3	1.3				0.52	122.7

Samples were knitted using four different types of yarn with similar yarn count and varying cover factor (CF).

The physical properties of the fabric samples tested are shown in *Table I.* The fabric samples were fitted to the cylinder with a constant tension resulting in a variable elongation (9%-56%).

In order to analyse the effect of fabric stretch and cover factor on stitch geometry and surface structure, images were captured of all test samples in both configurations with an Epson Perfection 3490 flatbed scanner. Areas of 20x20mm from the midlength of the fabric samples were scanned with a resolution of 2400ppi. The images were converted to binary images using a threshold value found by Otsu's method [20]. The number and average area of pores were then calculated in Matlab.

Drag Measurements

Drag force measurements were performed in a large scale wind tunnel in the aerodynamic lab at the Norwegian University of Science and Technology (NTNU). The tunnel is a closed circuit construction capable of producing wind speeds up to 25 m/s and the test section measures 12.5×2.7×1.8 meters. Drag forces were measured using a Schenck six component

force balance, logging only the stream wise force component. The test cylinder was placed 1.6 meters downstream of the test section inlet. The free-stream wind speed was measured using a pitot tube placed in the front of the test section and a pressure transducer. All data was acquired at 100Hz using custom LabView software.

A test PVC cylinder was fixed to the force balance with a stiff steel rod bolted to a solid steel support. This setup eliminated almost all vibrations in the cylinder. In order to reduce end effects around the cylinder edges, dummy cylinders were mounted both under and above the test cylinder. They were mounted as shown in *Figure 3* and were not clad with textiles during the experiments. Blockage ratio was calculated to 0.9% and could hence be disregarded. A disadvantage of the setup is the low distance from the tunnel floor to the test model which may cause the results to be influenced by the test sections boundary layer. During the experiments the test cylinder was clad with tube shaped fabric samples. The samples covered the whole cylinder section and any excess length fabric, due to variable longitudinal contraction, was folded and fixed leaving no loose fabric in the air flow.

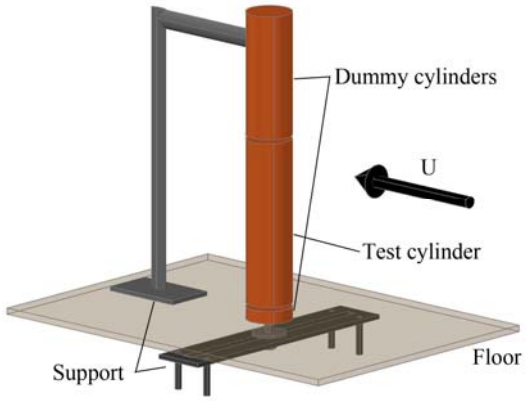

FIGURE 3. Wind tunnel setup for drag measurements.

Drag force measurements were performed for all fabric samples on a cylinder model of 65mm diameter. Varying wind speeds ranging from approximately 10-25 m/s were used. Measurements were made at 10 incremental points controlled by the fan RPM and data were acquired at 100Hz. In order to reduce influence from low frequency variations in the system, each measurement value was defined to be the average of the three median samples taken from a total of five samples of six seconds each. Standard deviations of the drag coefficient were calculated from all five samples. The current wind speed was calculated from the pressure difference measured by a pitot tube, and the air temperature in the tunnel was measured and averaged for every measurement series. A zero measurement was acquired prior to each series in order to ensure no influence from varying offset voltages between the measurements.

The cylinder model was completely covered by the fabric samples during the measurements and the seam of the sample was placed on the leeward side of the model.

PIV and Pressure Distribution Measurements

PIV recordings and measurements of the pressure distribution around the cylinder circumference were performed in a medium scale, closed circuit wind tunnel in the aerodynamics lab at the Norwegian University of Science and Technology (NTNU). The test section has cross sectional dimensions of 0.51(h) x 1.00(w) meters. The test setup is described in *Figure 4*. A PVC cylinder (D=65mm) was equipped with 18 pressure taps around the circumference at the half-length. The pressure taps were made from 1 mm steel tubes glued and aligned with the surface with a spacing of approx. 11 mm. Pressure tubes were connected to a Scanivalve feeding a single pressure to a pressure transducer. Hence the pressure data was not acquired simultaneously, but rather over a 10min time period.

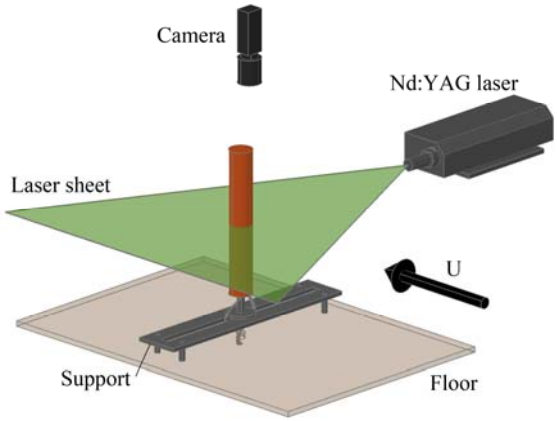

FIGURE 4. Wind tunnel setup for PIV and pressure distribution measurements.

The blockage ratio of this setup is 6.5%, and under the limit were blockage effects are usually considered. Significant influences of both blockage and aspect ratio on pressure distribution are however also reported for the values used in this study [21]. The data presented here are not corrected.

Particle Image Velocimetry (PIV) was utilized for analysis of the flow field in the cylinder wake. The method allows for high accuracy determination of the instantaneous flow field without interference with the flow. A detailed description of the PIV method can be found in I. Grants PIV-review[22]. A NewWave Solo Nd:YAG laser was used to create a thin horizontal oriented laser illumination sheet in the test section. Fog was injected to the flow with a Safex F2010 fog machine downstream of the test cylinder. A FlowSense M2 10 bit digital camera from Dantec Dynamics with a Nikon Nikkor 35mm F2.0 lens was mounted above the test section perpendicular to the laser sheet. The resulting field of view allowed half the wake to be captured in on frame. The half wake was then mirrored around the y-axis. An average velocity profile of the wake four diameters downstream of the cylinder was extracted from the acquired velocity field. A pixel resolution of 1600x1184 pixels gave a spatial resolution of approximately 10 pix/mm.

PIV and pressure probe experiments were conducted simultaneously on a 65mm cylinder model. CF1.0 and CF1.3 samples were used for this test session. 150 PIV recordings of the near wake were captured with a laser firing rate of 8 Hz to produce a 19 second average velocity field for each configuration. Four constant ranging from $5x10^4$ to $2.5x10^5$ were selected based on the C_D-Reynolds curves from the drag measurements.

It must be considered that the setup of the test cylinder and the cross section of the wind tunnel are different from the drag measurements. This influences both aspect ratio effects and blockage which may influence the onset of the drag crisis. Hence the C_D values and the state of the flow found from the pressure distribution may deviate somewhat from the corresponding drag measurements.

The discrete data from the pressure measurements around the cylinder circumference was interpolated using a cubic spline interpolation method and the drag was calculated from the interpolated data series.

RESULTS AND DISCUSSION

Surface Analysis

The amount and characteristics of fuzz (fiber ends) covering the surface are not quantitatively investigated but the qualitative differences can be observed in *Figure 5*. Samples made of spun yarn exhibit considerable surface fuzz-layers while the sample made of continuous filament polyester yarn has no apparent surface fuzz.

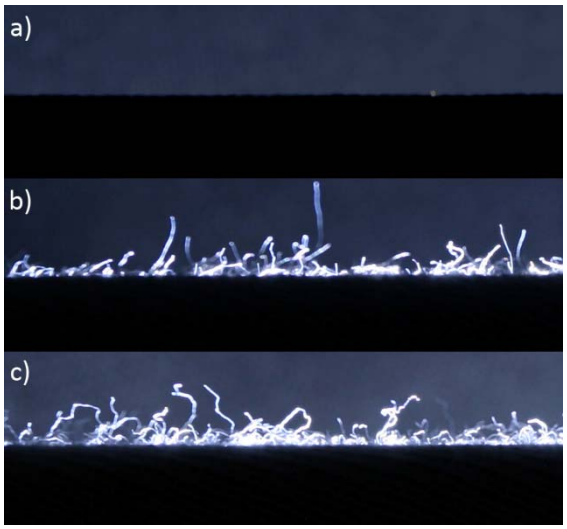

FIGURE 5. Profile images of PM (a), PS (b) and CS (c) textile samples. Depth of profile is 9mm.

FIGURE 6*Figure 6* demonstrates the optical porosity of the PM1.0 and PM1.4 filament polyester fabrics compared to the WS1.0 and WS 1.4 wool fabrics. It is clear from that the size of the areas not covered by yarn and the density of the samples themselves differ and are expected to influence the apparent surface roughness of the fabric. The high elasticity of the wool yarn makes the knit more porous for low cover factors since the tension is a constant parameter, but for high cover factors the wool knit stays more uniform under tension than the polyester knit.

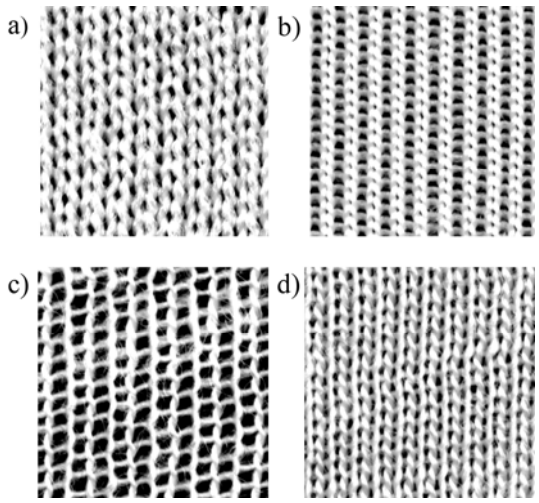

FIGURE 6. PM1.0 (a), PM1.4 (b), WS1.0 (c) and WS1.4 (d) samples of 7.5·7.5mm.

The size and number of pores of all tested samples are shown in *Figure 7* and *Figure 8*. The wool fabrics exhibit smaller and more numerous pores with

increasing cover factor in an almost linear relationship. This behavior can be expected as the loop length decreases with increasing cover factors. The other fabric samples however have a tendency to show fewer and larger pores for cover factors exceeding 1.2-1.3, and appear to exhibit a change in surface structure. The reason for this is that due to the gauge of the knitting machine being constant, the stitches contract and close the openings in the needle loops (making them smaller than 0.01mm^2) while the wales (sinker loops) extend and align horizontally, and thus reveal larger openings (*Figure 8*). This is seen as a distinct ribbing of the surface which will likely influence the aerodynamic behavior of the fabric. The wool fabrics do not seem to have this property. This could be due to the high elasticity of the wool fiber and the hairiness of the yarn.

It is clear that the change of the cover factor of the sample fabrics will influence not only optical porosity and surface roughness, but also their elastic properties of the fabrics, such as elastic deformation under stress and recovery. Thus, it is likely that the aerodynamic influence of fabric surface on the boundary layer cannot be predicted from cover factor alone.

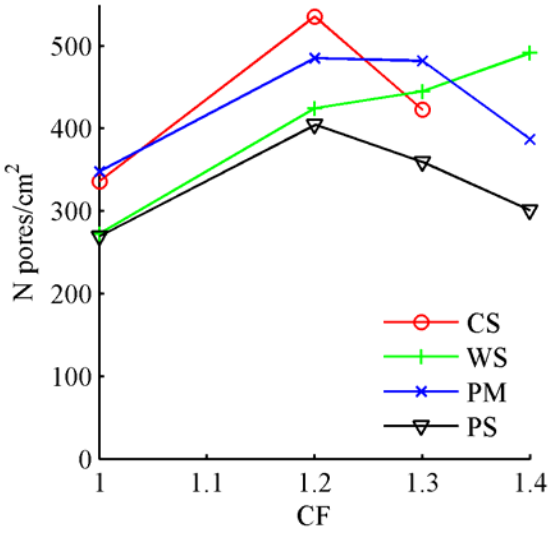

FIGURE 7. Average number of pores per cm^2 exceeding 0,01mm^2.

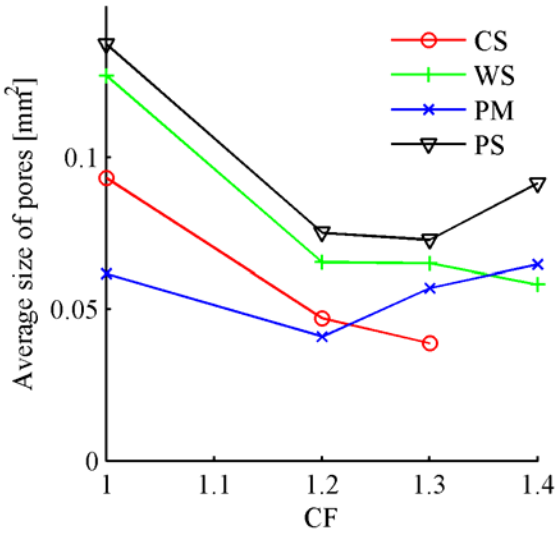

FIGURE 8. Average size of pores exceeding 0,01mm^2.

Drag Generated by Fabric Samples

The results of the drag measurements conducted on the force balance are presented as C_D vs. Reynolds number curves shown in *Figure 9*. In the subcritical regime all PM samples coincide at a C_D of approximately 0.8, also coinciding with the smooth cylinder, as expected since C_D is independent of surface roughness in this regime. The subcritical C_D value is however somewhat lower than the expected value of 1.2 sited in existing research [9, 13], and this may be caused by the fact that the cylinder model in the present study was placed near the floor of the tunnel test section, giving rise to possible boundary layer influence. Most noticeable from these results is however the apparent difference between the samples made of continuous filament yarn and of spun yarn. The results for PM fabrics correspond well with results from previous studies [5, 18] with rather abrupt transition causing a reduction of C_D. The samples made of spun yarns however do not show the expected drop in C_D in this range of Reynolds numbers, but rather exhibit a constant C_D over the whole range of Reynolds numbers, indicating that the fibers protruding from the fabric surface have a considerable influence on the flow field. Although the influence of cover factor on C_D is small, the samples with CF=1.00 appear to produce the highest

drag in general for all sample fabrics. The cylinders clad with fabrics made from spun yarn also show a C_D exceeding that of a smooth cylinder. This may be due to the additional drag induced by the fiber ends protruding from the fabric surface, and not the surface macro structure itself. Considering the resemblance between the filament fabrics and the spun fabrics found in the surface analysis (with the exception of wool fabrics) (*Figure 7 and Figure 8*) it is likely that the increased roughness caused by the "fuzz" will have tripped the transition to turbulence in the boundary layer at even lower Reynolds numbers, making the flow supercritical. It is most likely that the contribution of "fuzz drag", also found on tennis balls, increases the drag in this regime [17].

Results in *Figure 9* deviate from those of Oggiano et al. where a linear correlation between $Re_{critical}$ and CF was found [18]. The measurements in that study were however performed with negligible deformation of the fabrics samples (<1%), and consequently resulted in less influence from elastic deformation. If the results in presented in *Figure 9* are compared with the image analysis presented in the previous section it can be assumed that the critical Reynolds number is affected by the number and the size of depressions on the fabric surface where more numerous and smaller pores result in higher critical Reynolds numbers. This observation agrees well with the high $Re_{critical}$ found for the PM1.2 sample. No clear relationship can however be established from this analysis due to the additional influence of fabric elastic deformation. The occurrence of a ribbed pattern in a wale direction at higher cover factors is likely to affect the state of the boundary layer and makes this approach in defining roughness unreliable.

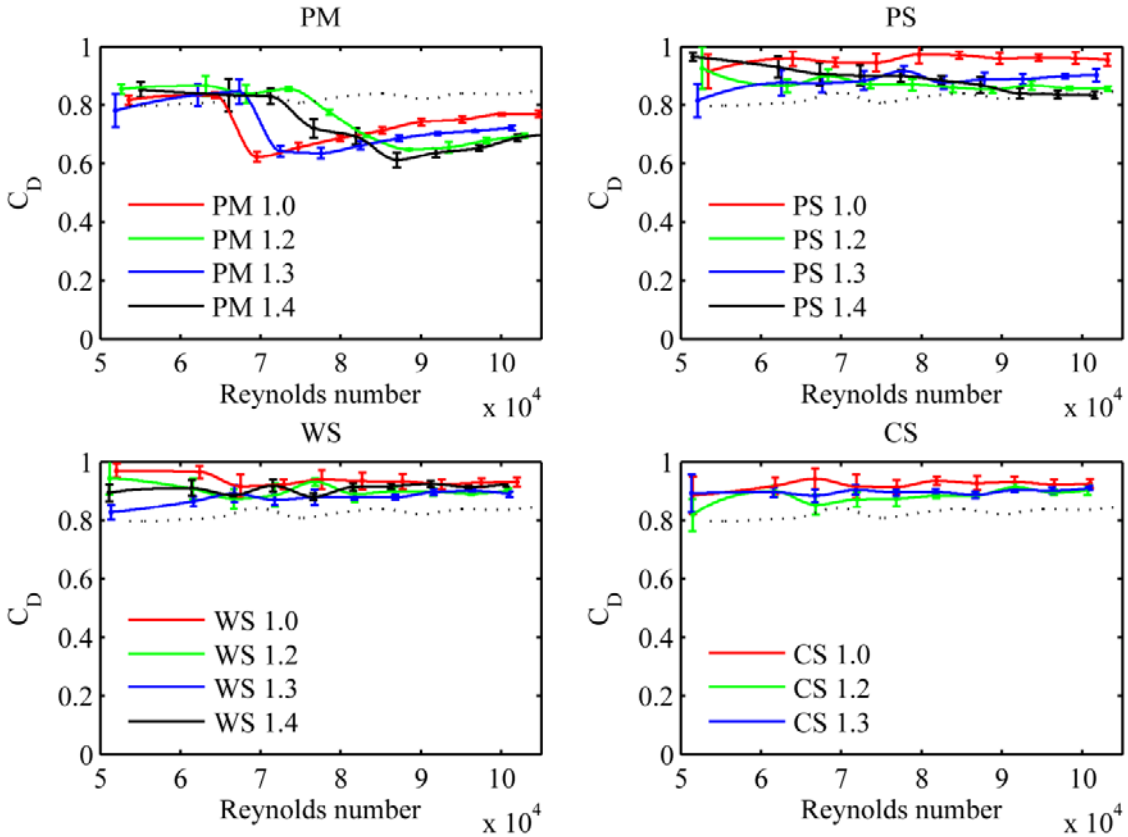

FIGURE 9. C_D vs. Reynolds number for 65mm cylinder with error bars (SD). Results for smooth cylinder included as dashed lines for comparison.

An interesting observation is that the wool samples have a rather linear relationship between their cover factor and the measured surface parameters. The effect of this on critical Reynolds number can however not be seen because of the influence of "fuzz". The poor agreement between cover factor and critical Reynolds number may be partially caused by the definition of cover factor which defined in relaxed state which does not account for elastic deformation of the sample on the cylinder. An analytical approach where the actual ratio between total sample area and net "yarn area" is measured as

proposed by Tàpias et al. may prove more useful [23]. Alternatively a roughness factor based on measured characteristic dimensions of the surface may also be a better suited estimate of the surface roughness of a fabric under tension [18].

The high scatter in the low Reynolds number range may be caused by the fact that the small test cylinder produced low drag forces at low wind speeds, giving a higher relative uncertainty. Hence a larger cylinder model would be preferred for better accuracy at subcritical speed.

Pressure Distribution

The mean pressure distribution around the cylinder model is presented as mean pressure coefficients (C_p) around the cylinder circumference in *Figure 10.* A leeward shift of the minimum pressure coefficient $C_{p\ min}$ and an increase of the average pressure coefficient in the separated region denoted C_{pb}, with increasing Reynolds number is accompanied by a reduction of pressure drag in the critical flow region. The concurrence of $C_{p\ min}$, maximum C_{pb}, maximum separation angle and drag crisis is clearly shown earlier by Güven et al. [24]. The consistency of the results and the good agreement with the smooth cylinder indicates that the air permeability of the fabric samples is large enough to allow undisturbed pressure readings of as assumed by D'Auteuil et. al[15].

The pressure distributions in *Figure 10* show that the PM fabrics undergo transition in this Reynolds range with a distinct reduction and leeward shift of $C_{p\ min}$. The base pressure coefficient is however nearly unchanged with the change of Reynolds number. In addition the values of $C_{p\ min}$ and C_{pb} are higher than values found for other rough cylinders in earlier studies [24-26].

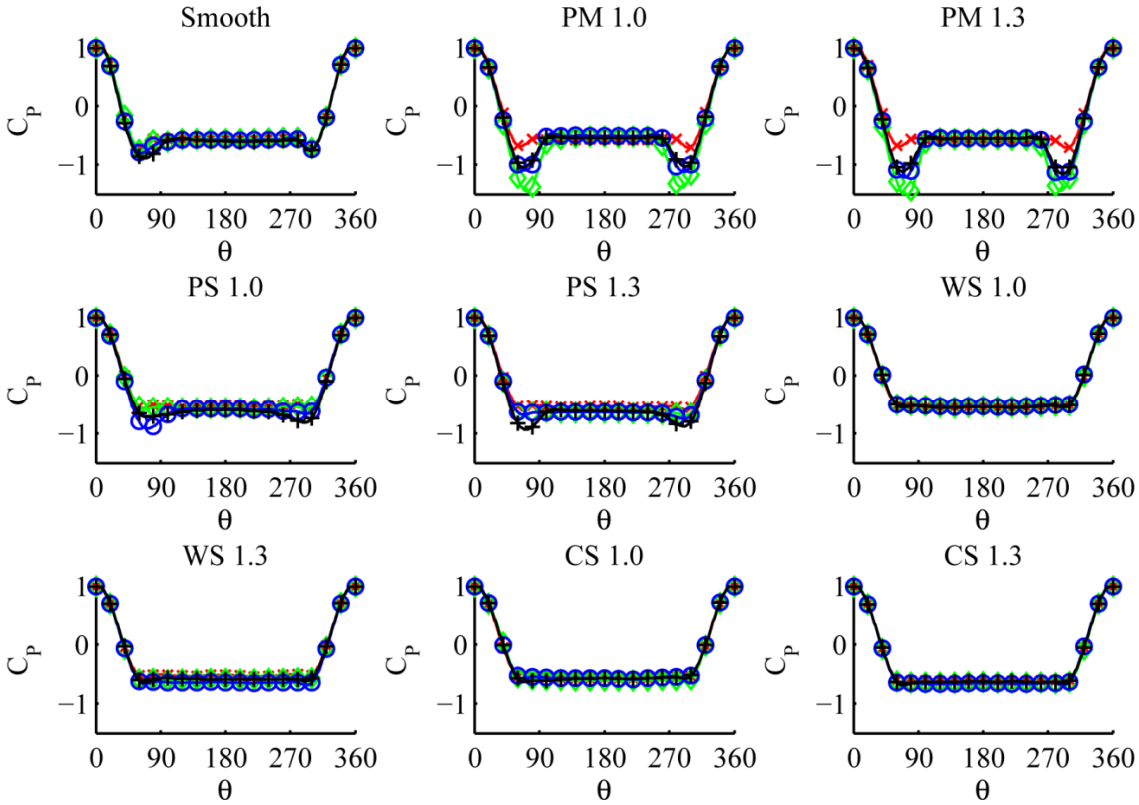

FIGURE 10. Pressure distribution around cylinder circumference. Red x: Re=5x10^4, green ◊: Re=7,5x10^4, blue o: Re=10^5, black +: Re=2,5x10^5.

The pressure distribution for the PM fabrics is similar to the smooth cylinder at the subcritical Reynolds number as this Reynolds region is known to be independent of roughness. The spun wool and cotton sample fabrics show next to no variance: neither with the change of cover factor nor with the change of Reynolds number. These fabrics seem to cause separation without any pressure recovery indicating that the boundary layer is considerably weakened prior to the onset of the adverse pressure gradient, causing early separation. It is possible that the "fuzz" makes the boundary layer thicker and hence weaker

prior to C_{pmin}. This is also the case for the PS samples at the lowest speed, but these samples have a lower $C_{p\ min}$ at higher Reynolds numbers. These samples also have a slightly asymmetrical pressure distribution at the higher Reynolds numbers. The differences found here all small and a reduction in drag was not observed in the drag measurements. The difference in pressure field found between PS samples and samples made of spun natural fibers is rather surprising, as no obvious difference is observed in the surface analysis. The natural softness of wool and cotton fibers contributes to a softer handle of these samples and indicates that the fiber surface "fuzz" might have different softness and distribution.

For comparison the average pressure distribution around the smooth cylinder is invariant as expected for the upper subcritical regime [14].

The adverse pressure gradient recovery can be expressed as C_{pb} - $C_{p\ min}$ and is closely related to the drag coefficient as both the lowest $C_{p\ min}$ and the highest C_{pb} is coinciding with the drag crisis[24]. This quantity is also known to be quite insensitive to influencing parameters like aspect ratio, blockage etc.[14]. The pressure recovery C_{pb} - $C_{p\ min}$ is plotted in *Figure 11* along with the C_D calculated from integration of C_P around the cylinder circumference. This demonstrates that the effect of the change in pressure distribution on drag for the PS samples is greatly reduced in comparison to the PM samples. The reason for this behavior can not, when compared to the drag measurements at the same Reynolds numbers, be assosiated with transition to turbulence in boundary layer. In comparison, the wool and cotton fabrics show no reduction in drag in this range of Reynolds numbers.

The polyester fabrics have similar drag coefficients for both cover factors tested at the measurement points, but the exact occurance of the drag crisis and the minimum C_D can not be located due to the low density of measurement points. C_D values found from pressure distributions corespond well with drag measurements and are somewhat lower than the values showed in *Figure 9* since the calculated values do not account for the friction drag.

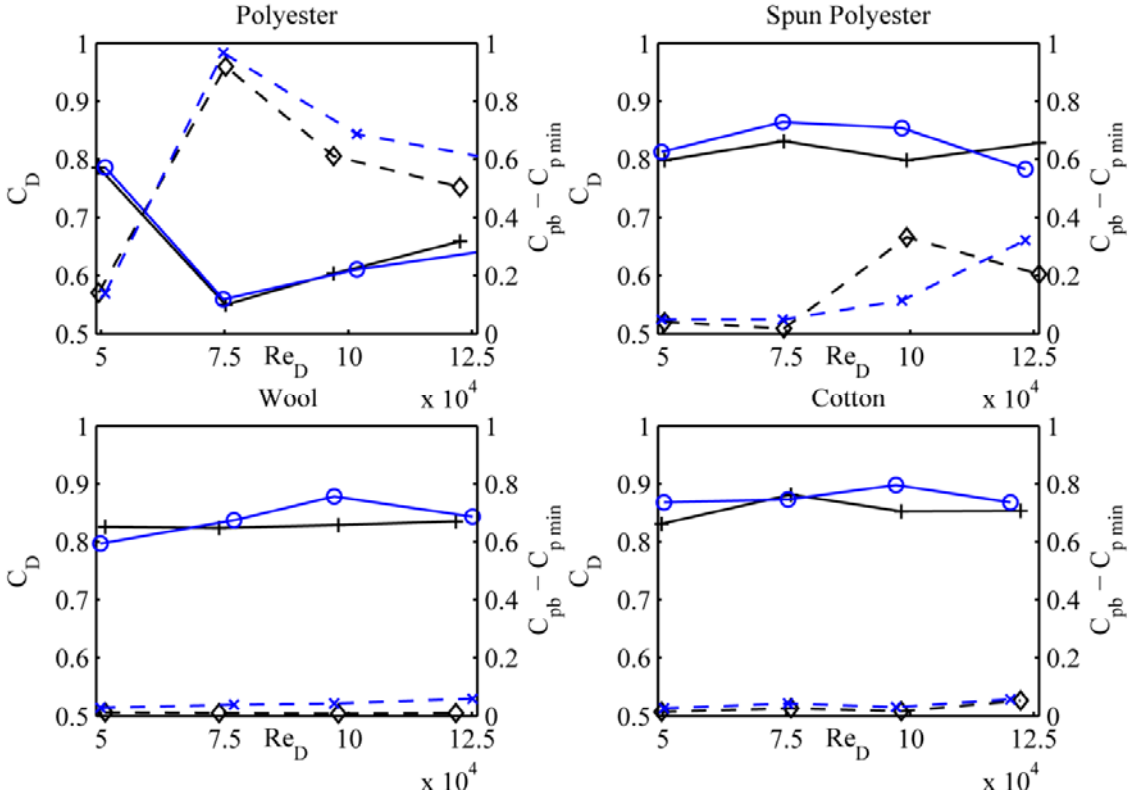

FIGURE 11. C_D calculated from pressure distribution (solid lines) and pressure recovery Cpb - Cp min (dashed lines). Black +: CF=1.0, blue o: CF=1.3, black ◊: CF=1.0, blue x: CF=1.3.

Wake Velocity Profiles

Velocity profiles of the stream-wise velocity component extracted from PIV recordings made in the near wake of the cylinder are presented in *Figure 12.* The profiles agree well with the pressure distributions with coinciding curves for the smooth cylinder and the wool and cotton clad cylinders. The Reynolds number dependency for PS fabrics found in the pressure distribution is also apparent here as a change in velocity defect. Boundary layer measurements should be applied in order to identify the reason for this behavior.

As expected the PM samples have lower velocity defects around the critical Reynolds number as a lower velocity defect in the wake is associated with higher pressure recovery around the cylinder and consequently a lower drag. The PM1.3 fabric has a lower velocity defect than the PM1.0 fabric at Re=75k, but it must again be noted that the low number of measurement points renders the exact determination of the minimum velocity defect impossible. It is also clear that the smooth cylinder has a lower velocity defect than all fabric-covered cylinders, with exception of the polyester-clad cylinders at high Reynolds numbers. This means that a smooth surface would cause a lower drag in the subcritical regime than a spun fabric surface in the supercritical regime. The fabrics made from spun yarns can hence be regarded as disadvantageous for all Reynolds numbers tested with respect to drag reduction.

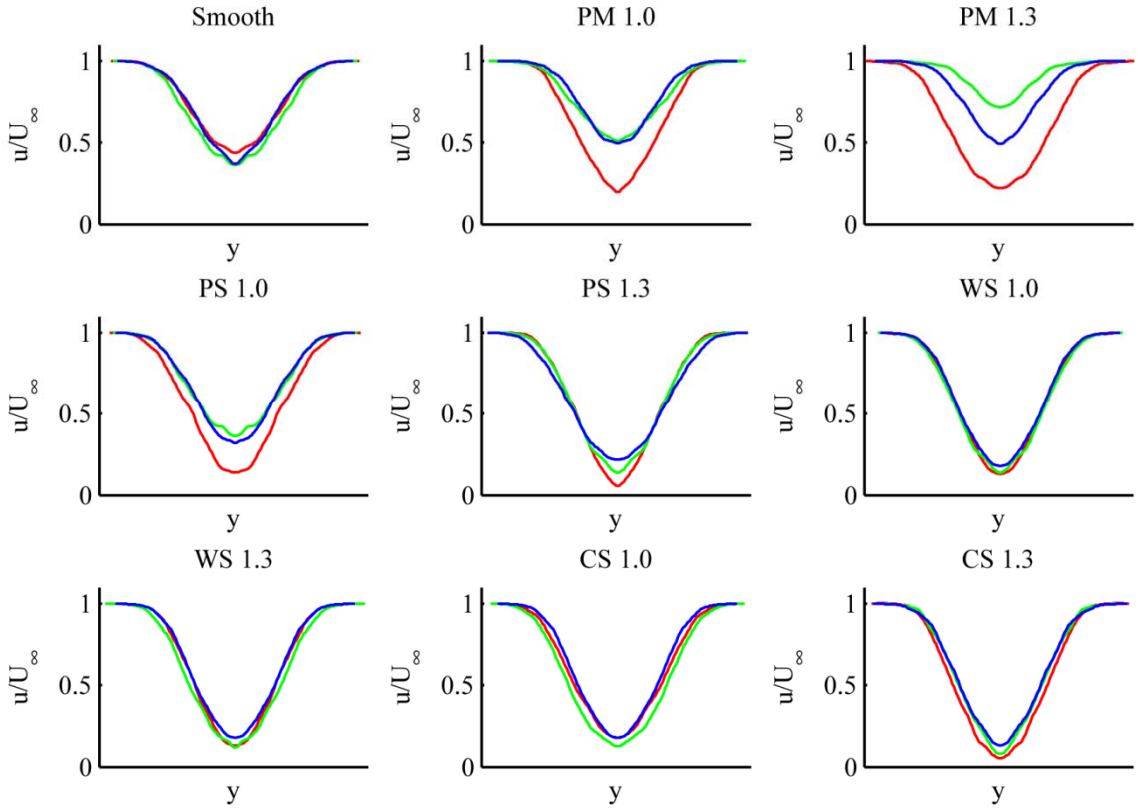

FIGURE 12. Mean wake velocity profiles at x/d=4. Red: Re=5x10^4, green: Re=7,5x10^4, blue: Re=10^5.

CONCLUSIONS

From the results shown in this paper it is obvious that the properties of the yarn composing the knitted fabrics have considerable influence on the flow field. A clear distinction was found between fabrics made from spun yarns and fabrics made from filament yarns. The aerodynamic properties of the filament polyester fabrics tested proved to show a clear dependence on fabric manufacturing parameters and elastic deformation, as opposed to the spun yarn fabrics which seem to be more influenced by the characteristics of the surface fiber "fuzz" layer. No significant connection between fabric cover factor, elastic deformation and drag could be found for the fabrics made from spun yarns. On a 65mm cylinder model only the filament polyester fabric caused a drag crisis in the range of Reynolds numbers tested, while the spun yarn fabrics showed constant C_D values. It appears that the fiber "fuzz" elements act to considerably complicate the flow with the

introduction of additional fuzz drag from the individual fiber elements and the dependence of fiber orientation in dynamic environments. In addition, the fabrics made from spun yarns gave a higher C_D compared to the smooth cylinder.

For the polyester fabrics an influence of elastic deformation on the critical Reynolds number could be observed. When the fabrics are elongated in the course-direction (direction of the yarn path) the change in knit structure appears to depend on cover factor. Higher cover factor fabrics tends to produce a ribbed surface when stretched, as opposed to fabrics of lower cover factor which remain more uniform. Based on this observation and the drag measurements, it appears that succession of drag crisis for stretched knitted fabrics cannot be solely determined by their cover factor.

When choosing appropriate fabrics for drag reducing purposes, the yarn used should preferably be smooth with no surface fiber "fuzz" elements influencing the flow. This will contribute to a potential higher drag reduction and leave the roughness of the fabric solely defined by the macro-structure of its surface.

REFERENCES

[1] F. Grappe, R. Candau, A. Belli, J.D. Rouillon, Aerodynamic drag in field cycling with special reference to the Obree's position, Ergonomics, 40 (1997) 1299 - 1311.

[2] G.J. van Ingen Schenau, The influence of air friction in speed skating, Journal of Biomechanics, 15 (1982) 449-458.

[3] L.W. Brownlie, Aerodynamic Characteristics of Sports Apparel, in, Simon Fraser, University of British Columbia, Canada, 1992.

[4] L. Oggiano, L. Sætran, S. Løset, R. Winther, Reducing the athlete's aerodynamical resistance, Journal of Computational and Applied Mechanics, 5 (2006).

[5] L. Brownlie, C. Kyle, J. Carbo, N. Demarest, E. Harber, R. MacDonald, M. Nordstrom, Streamlining the time trial apparel of cyclists: the Nike Swift Spin project, Sports Technology, 2 (2009) 53-60.

[6] L. Oggiano, L. Sætran, A low drag suit for ski-cross competitions, Procedia Engineering, 2 (2010) 2387-2392.

[7] E. Achenbach, Distribution of local pressure and skin friction around a circular cylinder in cross-flow up to Re = 5x106, Journal of Fluid Mechanics, 34 (1968) 625-639.

[8] J.R. Shanebrook, R.D. Jaszczak, Aerodynamic drag analysis of runners, Medicine and Science in Sports, 8 (1976) 43-47.

[9] C. Wieselsberger, New data on the laws of fluid resistance, Physikalishe Zeitschrift, 22 (1922).

[10] A. Fage, J.H. Warsap, The effects of turbulence and surface roughness on the drag of a circular cylinder, in, Aeronautical Research Committee, 1929.

[11] H.J. Niemann, N. Hölscher, A review of recent experiments on the flow past circular cylinders, Journal of Wind Engineering and Industrial Aerodynamics, 33 (1990) 197-209.

[12] A. Roshko, Experiments on the flow past a circular cylinder at very high Reynolds number, Journal of Fluid Mechanics, 10 (1961) 345-356.

[13] G. Schewe, On the force fluctuations acting on a circular cylinder in crossflow from subcritical up to transcritical Reynolds numbers, Journal of Fluid Mechanics, 133 (1983) 265-285.

[14] M.M. Zdravkovich, Flow around circular cylinders, Oxford University Press, 1997.

[15] A. D'Auteuil, G.L. Larose, S.J. Zan, Relevance of similitude parameters for drag reduction in sport aerodynamics, Procedia Engineering, 2 (2010) 2393-2398.

[16] D.J. Spencer, Knitting Technology - A Comprehensive Handbook and Practical Guide, 3rd ed., Woodhead Publishing, 2001.

[17] R.D. Mehta, J.M. Pallis, The aerodynamics of a tennis ball, Sports Engineering, 4 (2001) 177-189.

[18] L. Oggiano, O. Troynikov, I. Konopov, A. Subic, F. Alam, Aerodynamic behaviour of single sport jersey fabrics with different roughness and cover factors, Sports Engineering, 12 (2009) 1-12.

[19] E. Achenbach, E. Heinecke, On vortex shedding from smooth and rough cylinders in the range of Reynolds numbers 6x103 to 5x106, Journal of Fluid Mechanics, 109 (1981) 239-251.

[20] N. Otsu, A Threshold Selection Method from Gray-Level Histograms, IEEE Transactions on Systems, Man, and Cybernetics, 9 (1979) 62-66.

[21] G.S. West, C.J. Apelt, The effects of tunnel blockage and aspect ratio on the mean flow past a circular cylinder with Reynolds numbers between 104 and 105, Journal of Fluid Mechanics, 114 (1982) 361-377.

[22] I. Grant, Particle image velocimetry: a review, Proceedings of the Institution of Mechanical Engineers, Part C: Journal of Mechanical Engineering Science, 211 (1997) 55-76.

[23] M. Tapias, M. Rallo, J. Escofet, Fabric's cover factor measurement by image thresholding, in: A.M. O, J.L. Paz (Eds.), SPIE, 2004, pp. 229-232.
[24] O. Güven, C. Farell, V.C. Patel, Surface-roughness effects on the mean flow past circular cylinders, Journal of Fluid Mechanics, 98 (1980) 673-701.
[25] E. Achenbach, Influence of surface roughness on the cross-flow around a circular cylinder, Journal of Fluid Mechanics, 46 (1971) 321-335.
[26] J.P. Batham, Pressure distributions on circular cylinders at critical Reynolds numbers, Journal of Fluid Mechanics, 57 (1973) 209-228.

AUTHORS' ADDRESSES

Lars Morten Bardal
Luca Oggiano
Olga Troynikov
Inna Konopov
Norwegian University of Science and Technology (NTNU)
Kolbjørn Hejes vei 2
Trondheim 7491
NORWAY